Eur. Phys. J. C (2016) 76:444
DOI 10.1140/epjc/s10052-016-4288-1

THE EUROPEAN PHYSICAL JOURNAL C

Regular Article - Theoretical Physics

Static spherically symmetric wormholes in $f(R, T)$ gravity

M. Zubair[1,a], **Saira Waheed**[2,b], **Yasir Ahmad**[1,c]

[1] Department of Mathematics, COMSATS, Institute Of Information Technology, Lahore 54590, Pakistan
[2] Prince Mohammad Bin Fahd University, Al Khobar 31952, Kingdom of Saudi Arabia

Received: 18 May 2016 / Accepted: 26 July 2016 / Published online: 8 August 2016

Abstract In this work, we explore wormhole solutions in $f(R, T)$ theory of gravity, where R is the scalar curvature and T is the trace of stress-energy tensor of matter. To investigate this, we consider a static spherically symmetric geometry with matter contents as anisotropic, isotropic, and barotropic fluids in three separate cases. By taking into account the Starobinsky $f(R)$ model, we analyze the behavior of energy conditions for these different kinds of fluids. It is shown that the wormhole solutions can be constructed without exotic matter in few regions of space-time. We also give the graphical illustration of the results obtained and discuss the equilibrium picture for the anisotropic case only. It is concluded that the wormhole solutions with anisotropic matter are realistic and stable in this theory of gravity.

1 Introduction

After Hubble's theory of the expanding universe, current observations from Supernovae Type Ia and CMBR (Cosmic Microwave Background Radiation) [1–3] have confirmed the phenomenon of the accelerated expanding universe. The modified theories are quite useful in the present era because these theories can help to explain the possible cosmic expansion history and its related concepts. In this context, $f(R)$ theory has appeared as one of the first and simplest modifications to the Einstein–Hilbert action. This theory has been extensively employed to discuss the dark energy (DE) and mainly the accelerating cosmic expansion [4]. Furthermore, the $f(R)$ theory of gravitation provides us with the scenarios of early time inflation and late time expansion of the accelerated universe [5]. The features of DE and late time cosmic acceleration are also explained in some other modified theories of gravity such as $f(\tau)$ (where "τ" is for the torsion) [6,7], Gauss–Bonnet gravity [8,9], Brans–Dicke theory [10] and $f(T, T_G)$, [11], etc.

A few years ago, Harko et al. [12] introduced a modification to Einstein's gravity and named it the $f(R, T)$ theory of gravity. This was basically an extension to $f(R)$ gravity obtained by introducing the trace "T" of the energy-momentum tensor together with the Ricci scalar "R". Furthermore, they derived the corresponding field equations from the coupling of matter and geometry in the metric formalism for some specific cases. Recently, Houndjo [13] reconstructed some cosmological models of the form $f(R, T) = f_1(R) + f_2(T)$, in the presence of an auxiliary scalar field with two known examples of the scale factor that correspond to an expanding universe. In [14], the authors considered cosmological scenarios based on $f(R, T)$ theories of gravity and numerically reconstructed the function $f(R, T)$ for a holographic DE model that can reproduce the same expansion history as generated in general relativity (GR). Till the present time, different cosmological aspects have been addressed in $f(R, T)$ gravity including reconstruction schemes, anisotropic solutions, energy conditions, thermodynamics, viscous solutions, phase space perturbations and stability, etc. [15–32].

Wormholes are hypothetical topological features that provide a subway for different space-times apart from each other. In 1935, Einstein and Rosen [33] were first to obtain the wormhole solutions known as Lorentzian wormholes or Schwarzschild wormholes. Wormholes are of two kinds: static wormholes and dynamic wormholes. Normally, an exotic fluid is needed for the formation of static wormholes which violates the NEC in GR. Lobo and Oliveira [34] explained the fact that wormhole solutions can be formed without violation of energy conditions, *i.e.*, WEC and NEC, in $f(R)$ theory of gravity. They reconstructed $f(R)$ by considering a trace-less fluid and equations of state for some particular shape function, to discuss the evolution of energy conditions.

[a] e-mails: mzubairkk@gmail.com; drmzubair@ciitlahore.edu.pk
[b] e-mail: swaheed@pmu.edu.sa
[c] e-mail: yasirahmad6667@gmail.com

In [35], the behavior of ordinary matter was studied to check whether it can support wormholes in $f(R)$ theory. For this purpose, WEC and NEC were analyzed in anisotropic, barotropic, and isotropic fluids and it was observed that the barotropic fluid satisfies these conditions in some certain regions of the space-time, while for the other two fluids, these conditions were violated. So, wormhole solutions can be obtained without exotic matter in a few regions of space-time only, without violating the energy conditions which are necessary for the existence of wormhole solutions in GR [36,37]. Recently, the wormhole geometries were studied in $f(R,T)$ gravity [38] by taking a particular equation of state (EoS) for the matter field into account. They showed that an effective stress-energy is responsible for the violation of the NEC.

Here, we are interested in finding wormhole solutions by introducing additional matter contributions in the $f(R)$ model (without involving any form of exotic matter). We analyze the behavior of the shape function, WEC, and NEC to explore the suitable regions for existence of wormhole solutions using anisotropic, barotropic, and isotropic fluids. This paper has the following organization. In Sect. 2, we present a short introduction of $f(R,T)$ gravity by developing the field equations. Section 3 relates to the discussion of wormhole geometries in the $f(R,T)$ theory of gravity for three types of fluids. Finally, Sect. 4 comprises the concluding remarks.

2 $f(R,T)$ Gravity

Here, we will give a short introduction to $f(R,T)$ theory of gravity. In his pioneering work, Harko et al. presented a new generalization of $f(R)$ gravity by taking the coupling of the Ricci scalar with the matter field into account as follows [12]:

$$\mathcal{I}=\int \mathrm{d}x^4\sqrt{-g}\,[f(R,T)+\mathcal{L}_{\mathrm{m}}]. \tag{1}$$

In the above action, $f(R,T)$ represents a generic function of the Ricci scalar R and the energy-momentum tensor trace $T=T^{\mu}_{\mu}$. Here, in the action, we have assumed gravitational units, i.e., $c=8\pi G=1$ and also the matter ingredients are introduced by the Lagrangian density $\mathcal{L}_{(\mathrm{matter})}$. This theory is considered as more successful as compared to $f(R)$ gravity in the sense that such a theory can include quantum effects or imperfect fluids that are neglected in a simple $f(R)$ generalization of GR. The variation of the metric $g_{\mu\nu}$ of the above action leads to the following set of field equations:

$$R_{\mu\nu}f_R(R,T)-\frac{1}{2}g_{\mu\nu}f(R,T)+\left(g_{\mu\nu}\Box-\nabla_{\mu}\nabla_{\nu}\right)f_R(R,T) = T_{\mu\nu}-f_T(R,T)\Theta_{\mu\nu}-f_T(R,T)T_{\mu\nu}. \tag{2}$$

This set involves derivative operators like ∇ and $\Box$, which represent the covariant derivative and the four-dimensional Levi-Civita covariant derivative also known as the d'Alembert operator, respectively. Also, the notations $f_R(R,T)$ and $f_T(R,T)$ correspond to derivatives of $f(R,T)$ with respect to the Ricci scalar, i.e., $\frac{\partial f(R,T)}{\partial R}$ and the energy-momentum, i.e., the trace $\frac{\partial f(R,T)}{\partial T}$, respectively. The term $\Theta_{\mu\nu}$ is defined by

$$\Theta_{\mu\nu}=\frac{g^{\alpha\beta}\delta T_{\alpha\beta}}{\delta g^{\mu\nu}}=-2T_{\mu\nu}+g_{\mu\nu}\mathcal{L}_m-2g^{\alpha\beta}\frac{\partial^2\mathcal{L}_m}{\partial g^{\mu\nu}\partial g^{\alpha\beta}},$$

where the matter energy-momentum tensor is introduced which is given by the following equation [39]:

$$T^{(m)}_{\mu\nu}=-\frac{2}{\sqrt{-g}}\frac{\delta(\sqrt{-g}\mathcal{L}_m)}{\delta g^{\mu\nu}}=g_{\mu\nu}\mathcal{L}_m-\frac{2\partial\mathcal{L}_m}{\partial g^{\mu\nu}}. \tag{3}$$

Here the second part of the above equation can be obtained, if the matter Lagrangian is assumed to depend only on the metric tensor rather than on its derivatives.

The source of the anisotropic fluid is defined by the following energy-momentum tensor:

$$T_{\mu\nu}=(\rho+p_r)V_{\mu}V_{\nu}-p_t g_{\mu\nu}+(p_r-p_t)\chi_{\mu}\chi_{\nu},$$

where V_{μ} is the 4-velocity of the fluid defined as $V^{\mu}=e^{-a}\delta^{\mu}_0$ satisfying $V^{\mu}V_{\mu}=1$ and $\chi^{\mu}=e^{-b}\delta^{\mu}_1$ gives $\chi^{\mu}\chi_{\mu}=-1$. Herein, we choose $\mathcal{L}_{(\mathrm{matter})}=\rho$, then the expression for $\Theta_{\mu\nu}$ takes the following form:

$$\Theta_{\mu\nu}=-2T_{\mu\nu}+\rho g_{\mu\nu}.$$

Consequently, the field equation (2) can be expressed as effective Einstein field equations of the form

$$R_{\mu\nu}-\frac{1}{2}Rg_{\mu\nu}=T^{\mathrm{eff}}_{\mu\nu}, \tag{4}$$

where $T^{\mathrm{eff}}_{\mu\nu}$ is the effective energy-momentum tensor in $f(R,T)$ gravity which is defined by

$$T^{eff}_{\mu\nu}=\frac{1}{f_R(R,T)}\Big[(1+f_T(R,T))T_{\mu\nu}-\rho g_{\mu\nu}f_T(R,T)+\frac{1}{2}(f(R,T)-Rf_R(R,T))g_{\mu\nu}+(\nabla_{\mu}\nabla_{\nu}-g_{\mu\nu}\Box)f_R(R,T)\Big]. \tag{5}$$

3 Wormhole geometries with three different matter contents

In this section, we will discuss static spherically symmetric wormholes with three types of matter contents: anisotropic,

isotropic, and barotropic. Consider a line element that describes a static spherically symmetric geometry of the form

$$ds^2 = e^{a(r)}dt^2 - e^{b(r)}dr^2 - r^2(d\theta^2 + sin^2\theta d\phi^2), \tag{6}$$

where $a(r)$ is an arbitrary function of r and for the wormhole geometry, we have $e^{-b(r)} = 1-\beta(r)/r$. The terms $a(r)$ and $\beta(r)$ represent the redshift function, and the shape function, respectively [36,37]. For the surface vertical to the wormhole throat, we must have a minimum radius at $r = \beta(r_0) = r_0$, then it increases from r_0 to $r \to \infty$. An important condition to have a typical wormhole solution is the flaring out condition of the throat, given by $\frac{(\beta-\beta' r)}{\beta^2} > 0$ and, moreover, $\beta(r)$ needs to meet the condition $\beta'(r_0) < 1$, which is imposed at the throat $\beta(r_0) = r = r_0$. In GR, these conditions give hints for to the existence of an exotic form of matter which requires the violation of the NEC. Also, the condition $1-\beta(r)/r > 0$ needs to be satisfied.

The field equations can be rearranged to find the expressions for ρ, p_r and p_t as follows:

$$\rho = \frac{1}{e^b}\left[\left(\frac{a'}{r} - \frac{a'b'}{4} + \frac{a''}{2} + \frac{a'^2}{4}\right)f_R(R,T) + \left(\frac{b'}{2} - \frac{2}{r}\right)f'_R(R,T) - f''_R(R,T) - \frac{f(R,T)}{2}e^b\right], \tag{7}$$

$$p_r = \frac{1}{e^b(1+f_T(R,T))}\left[\left(\frac{b'}{r} - \frac{a'b'}{4} - \frac{a''}{2} - \frac{a'^2}{4}\right)f_R(R,T) + \left(\frac{a'}{2} + \frac{2}{r}\right)f'_R(R,T) + \frac{f(R,T)}{2}e^b\right] - \frac{\rho f_T(R,T)}{(1+f_T(R,T))}, \tag{8}$$

$$p_t = \frac{1}{e^b(1+f_T(R,T))}\left[\left(\frac{(b'-a')r}{2} - e^b + 1\right)\frac{f_R(R,T)}{r^2} + \left(\frac{a'-b'}{2} + \frac{1}{r}\right)f'_R(R,T) + f''_R(R,T) + \frac{f(R,T)}{2}e^{b(r)}\right] - \frac{\rho f_T(R,T)}{(1+f_T(R,T))}. \tag{9}$$

It can be observed that the above equations appeared to be much complicated to find the explicit expressions of ρ, p_r, and p_t, since $f(R,T)$ has a direct dependence on the trace of the stress-energy tensor. In this scenario, we find that the only possibility left is to choose the function as $f(R,T) = f(R) + f(T)$ with $f(T) = \lambda T$, λ being the coupling parameter. Here, we set this choice for $f(R,T)$ and simplify Eqs. (7)–(9) as follows:

$$\rho = \frac{1}{2(1+2\lambda)}\left[\frac{2+5\lambda}{(1+\lambda)}Z_1 + \lambda Z_2 + 2\lambda Z_3\right], \tag{10}$$

$$p_r = \frac{-1}{2(1+2\lambda)}\left[\frac{\lambda}{(1+\lambda)}Z_1 - (2+3\lambda)Z_2 + 2\lambda Z_3\right], \tag{11}$$

$$p_t = \frac{-1}{2(1+2\lambda)}\left[\frac{\lambda}{(1+\lambda)}Z_1 - (2+3\lambda)Z_2 + 2\lambda Z_3\right], \tag{12}$$

where

$$Z_1 = \frac{1}{e^b}\left[\left(\frac{a'}{r} - \frac{a'b'}{4} + \frac{a''}{2} + \frac{a'^2}{4}\right)f_R + \left(\frac{b'}{2} - \frac{2}{r}\right)f'_R - f''_R - \frac{f}{2}e^b\right],$$

$$Z_2 = \frac{1}{e^b(1+\lambda)}\left[\left(\frac{b'}{r} + \frac{a'b'}{4} - \frac{a''}{2} - \frac{a'^2}{4}\right)f_R + \left(\frac{a'}{2} + \frac{2}{r}\right)f'_R + \frac{f}{2}e^b\right],$$

$$Z_3 = \frac{1}{e^b(1+\lambda)}\left[\left(\frac{(a'-b')r}{2} - e^b + 1\right)\frac{-f_R}{r^2} + \left(\frac{a'-b'}{2} + \frac{1}{r}\right)f'_R + f''_R + \frac{f}{2}e^b\right].$$

In [40,41], the authors have presented the study of energy conditions in $f(R,T)$ gravity. We recommend the readers to study to these papers for gaining an overview of this subject. As for the other modified theories, the violation of the NEC in $f(R,T)$ gravity imposes the condition $T^{eff}_{\mu\nu}\kappa^\mu\kappa^\nu < 0$, that is, $\rho^{eff} + p^{\text{eff}} < 0$. Here, we find the following expression:

$$\rho^{\text{eff}} + p_r^{\text{eff}} = \frac{1}{f_R}(\rho + p_r)(1+\lambda) + \frac{1}{f_R}\left(1 - \frac{\beta}{r}\right) \times \left(f''_{RR} + f'_R\frac{\beta - \beta' r}{2r^2(1-\frac{\beta}{r})}\right).$$

Using the field equations, this leads to

$$\rho^{\text{eff}} + p_r^{eff} = \frac{1}{r^3}\left(\beta' r - \beta\right),$$

which is similar to that in $f(R)$ gravity. Here, if we use the flaring out condition $\frac{(\beta-\beta' r)}{\beta^2} > 0$, it results in $\rho^{\text{eff}} + p^{\text{eff}} < 0$. In this case, we have kept NEC satisfied for matter energy tensor; however, the additional curvature components which arise due to the modification of Einstein's gravity play a role for the violation of the NEC.

In this study, we take a specific $f(R)$ model representing an R^n extension of the well-known Starobinsky model, and is it given by [42]

$$f(R) = R + \alpha R^2 + \gamma R^n,$$

where $n \geqslant 3$, α, and γ are arbitrary constants. The choice of $\alpha = \gamma = 0$ implies the Λ correction to GR. Basically, we want to take a power law model that should be singularity free

Table 1 Shape functions corresponding to different choices of parameter m

m	$m=1$	$m=1/2$	$m=1/5$	$m=0$	$m=-1/2$	$m=-3$
Shape Functions $\beta(r)$	r_0^2/r	$r_0\sqrt{r_0/r}$	$r_0^{6/5}r^{-1/5}$	r_0	$\sqrt{r_0 r}$	$r_0^2 r^3$

as well as it should be the generalization of linear models that are used in most of the literature for wormhole discussions. In the literature [43], it is pointed out that the power law models are always of great interest, e.g., $f(R)=\xi R^n$ with ξ, n any constants. In this model, there exists big rip singularities for a negative range of n. They also argued that if we impose $n>1$ with positive ξ, then $f(R)\to\infty$ only when $R\to\infty$. Thus, under these conditions, the possible presence of a singularity can be avoided. Further, in the literature, another form of Starobinsky model with disappearing cosmological constant is defined, $f(R)=R+\lambda R_0[(1+\frac{R^2}{R_0})^{-n}-1]$ [45]. Clearly, this model suffers the singularity problem. However, they also claimed that this singularity can be cured by adding a term $\propto R^2$ [44]. It can easily be seen that present Starobinsky model has a different form involving one R^2 term, therefore our used model does not suffer from any singularity problem. One can explore another viable $f(R)$ model, named the Hu–Sawicki model to present interesting cosmic features [46].

For this model, the field equations (10)–(12) take the form

$$\begin{aligned}\rho=&\frac{e^{-b}}{4r^2(1+\lambda)(1+2\lambda)}\Big[(1+2\alpha R+n\gamma R^{n-1})(2r^2a''\\&\times(1+2\lambda)-a'r(1+2\lambda)\\&\times\big(rb'-4\big)+r^2a'^2(1+\lambda)+4rb'\lambda+4\lambda(e^b-1))\\&+(2\alpha+n(n-1)\gamma R^{n-2})\\&\times\big(3r^2a'\lambda+r(2+3\lambda)(rb'-4)R'\\&-2r^2Re^b(1+\lambda)(R+\alpha R^2+\gamma R^n)-2r^2\\&\times\big(2+3\lambda)(\gamma n(n-1)(n-2)R^{n-3}R'^2+2\alpha R''\\&+\gamma n(n-1)R^{n-2}R''\Big],\end{aligned}\tag{13}$$

$$\begin{aligned}p_r=&\frac{e^{-b}}{4r^2(1+\lambda)(1+2\lambda)}\\&\times\Big[\big(1+2\alpha R+n\gamma R^{n-1}\big)\big(-4\big(-1+e^b\big)\lambda\\&+r\big(-(r+2r\lambda)a'^2+4(1+\lambda)b'+r(1+2\lambda)a'b'\\&-2r(1+2\lambda)a''\big)\big)+r\big(\big(2\alpha+n(n-1)\gamma R^{n-2}\big)\\&\times\big(8+12\lambda+r(2+\lambda)a'+r\lambda b'\big)R'\\&+2r\big(e^b(1+\lambda)\big(R+\alpha R^2+\gamma R^n\big)\\&-2\alpha\lambda R''-n(n-1)\gamma\lambda R^{n-3}\big((n-2)R'^2+RR''\big)\big)\big)\Big],\end{aligned}\tag{14}$$

$$\begin{aligned}p_t=&\frac{e^{-b}}{4r^2\big(1+3\lambda+2\lambda^2\big)}\Big[2\big(1+2\alpha R+n\gamma R^{n-1}\big)\\&\times\big(2\big(e^b-1\big)(1+\lambda)-(r+2r\lambda)a'+rb'\big)\\&+r\big(\big(2\alpha+n(n-1)\gamma R^{n-2}\big)\\&\times\big(4(1+\lambda)+r(2+\lambda)a'-r(2+3\lambda)b'\big)R'+2r\\&\times\big(e^b(1+\lambda)\big(R+\alpha R^2+\gamma R^n\big)+(2+3\lambda)\big(n(n-1)\\&\times(n-2)\gamma R^{n-3}R'^2+2\alpha R''+n(n-1)\gamma R^{n-2}R''\big)\big)\Big].\end{aligned}\tag{15}$$

In the further discussion, we take a particular value for $n, n=3$. Moreover, the redshift function is chosen to be constant with $a'(r)=0$. In coming sections, we discuss the energy bounds for three different fluid configurations.

3.1 Anisotropic fluid

Initially, we consider the anisotropic fluid model with the following choice of the shape function [47–54]:

$$b(r)=-\ln\left[1-\left(\frac{r_0}{r}\right)^{m+1}\right],\tag{16}$$

where m and r_0 are arbitrary constants. Since $e^{-b(r)}=1-\beta(r)/r$, in our case, Eq. (16) implies the following form of the shape function:

$$\beta(r)=\frac{(r_0)^{m+1}}{r^m}.\tag{17}$$

Clearly, $\beta(r)$ is characterized on the basis of m and can result in different forms, which have been explored in the literature as shown in Table 1. Here, $\beta(r)$ satisfies the necessary conditions for the existence of the shape function. To meet the flaring out condition $\beta'(r)<1$, one needs to set $m<1$. Also, the constraint $\beta(r_0)=r_0$ is trivially satisfied. Moreover, this shape function also satisfies the condition for an asymptotically flat space-time, i.e., $\beta(r)/r=r_0^{1-m}r^{m-1}\to 0$ as $r\to\infty$.

In [35], Lobo and Oliveira discussed the wormhole geometries in $f(R)$ gravity using the above defined shape function for the choices: $m=1$ and $m=-1/2$. Recently, Pavlovic and Sossich [49] discussed the existence of wormholes without exotic matter in different $f(R)$ models employing this shape function (16) with $m=1/2$.

Substituting $b(r)$ in Eqs. (13)–(15), we obtain

$$\rho = \frac{r_0 m}{r^9(1+\lambda)(1+2\lambda)}\left(\frac{r_0}{r}\right)^m\Bigg[-r^4\Big(r^2(1+2\lambda)+2(2+m)(3+m)\alpha(2+3\lambda)\Big)+r_0\left(\frac{r_0}{r}\right)^m r\Big(-12m(3+m)(5+2m)\gamma(2+3\lambda)+r^2\alpha\Big(30+26m+6m^2+45\lambda+9m\lambda(4+m)\Big)\Big)+2\gamma r_0^2 m\left(\frac{r_0}{r}\right)^{2m}\Big(m(154+226\lambda)+(15m^2+99)\times(2+3\lambda)\Big)\Bigg], \tag{18}$$

$$p_r = \frac{r_0}{r^9(1+\lambda)(1+2\lambda)}\left(\frac{r_0}{r}\right)^m\times\Bigg[-r^4\Big(r^2(1+2\lambda)+2m\alpha(3+m)(4+10\lambda+m\lambda)\Big)+2r_0^2m^2\left(\frac{r_0}{r}\right)^{2m}\gamma\times\Big(33(2+7\lambda)+m(20+(122+15m)\lambda)\Big)+r_0m\left(\frac{r_0}{r}\right)^m r\Big(-12m\gamma(3+m)(4+(13+2m)\lambda)+r^2\alpha\Big(20+55\lambda+m(6+(28+3m)\lambda)\Big)\Big)\Bigg], \tag{19}$$

$$p_t = \frac{r_0}{2r^9(1+\lambda)(1+2\lambda)}\left(\frac{r_0}{r}\right)^m\Bigg[-4r_0^2m^2\left(\frac{r_0}{r}\right)^{2m}\gamma\times\Big(231+169m+30m^2+(3+m)\times(121+45m)\lambda\Big)+r^4\Big((1+m)r^2(1+2\lambda)+4m(3+m)\alpha(6+10\lambda+m(2+3\lambda))\Big)+2r_0m\left(\frac{r_0}{r}\right)^m r\Big(-r^2\alpha\Big(40+65\lambda+m(16+3m)(2+3\lambda)\Big)+12m\gamma(3+m)\Big(12+19\lambda+m(4+6\lambda)\Big)\Big)\Bigg]. \tag{20}$$

In the following discussion, we present the suitable choice of the parameters for the viability of WEC: $\rho > 0$ and NECs: $\rho + p_r > 0$, $\rho + p_t > 0$. We compare the different shape functions depending on the choice of parameter m.

- $\beta(r) = r_0\sqrt{\frac{r_0}{r}}$

Here, we fix $r_0 = 1$ and $m = 1/2$ and discuss the viability ranges of α, γ, and r for two cases of the coupling constant, $\lambda > -1$ and $\lambda < -1$. In the case of the WEC, we find the following constraints:

- For $\lambda < -1$, WEC is valid if $r \geq 3$ and $\alpha \geq 15$, here r depends on the choice of α, for very large α, we can increase the validity region. However, r obeys the initial bound $r \geq 1.3$ for greater values of α. In the left plot of Fig. 1, we show the evolution of WEC versus α, γ, and r for $\lambda = -2$. One can see that there are some small regions where WEC is also valid for $\alpha < 0$. For the choice of a small of r, we refer the reader to the right plot in Fig. 1. We have shown the plot for $\lambda = -2$, it can be seen that there some small regions of validity involving $\alpha < 0$ and a very small range of r.
  - For a small region like $0 < r \leq 1$, we require $\gamma \leq -30$ and for $1 < r < 3$, we require $\alpha > 0$ with $\gamma \geq 30$.
- For $\lambda > -1$, the validity of WEC needs $\alpha \leq -20$ and $r \geq 2.8$. In left plot of Fig. 2, we have shown the validity regions for $\lambda = 2$, it can be seen that there some small regions of validity involving $\alpha > 0$ and a very small range of r. In the right plot of Fig. 2, we show the evolution for small ranges of r and find the following constraints:
  - For a small region, like $0 < r < 1$, we require $\gamma \geq 20$ and for $1.2 \leq r < 2.8$, the validity needs negative values of both α and γ.

Now we discuss the validity regions for $\rho + p_r > 0$ and $\rho + p_t > 0$. Again we develop two cases, depending on the choice of λ.

- For $\lambda < -1$, $\rho + p_r > 0$ is valid in the following regions: $0 < r < 1$ with $\gamma \leq -13$; $r \geq 1.1$ with $\alpha > 0$ and $\gamma > -1$; $r \geq 3$ with $\alpha \geq 10$.
- The validity of $\rho + p_t > 0$ can be met for three cases, i.e.,
  $0 < r < 1$ with $\gamma \geq 15$; $r \geq 1.1$ with $\alpha \leq -10$, and $\gamma < 0$; if $r \geq 3$ with $\alpha \leq -10$.

Now we present the constraints for $\lambda > -1$.

- Here, $\rho + p_r > 0$ can be satisfied for four different ranges depending on the choice of r: if $0 < r < 1$ with $\gamma \geq 15$; if $r \geq 2.9$, $\alpha \leq -15$; if $1 < r < 2.9$, $\alpha < 0$, $\gamma < 0$ and if $r \geq 1.1$ with $\gamma < 0$ and $\alpha \leq -10$.
- In the case of $\rho + p_t > 0$, we can find the validity for the following choices of the parameters: For $0 < r < 1$ with $\gamma \leq -16$; for $r \geq 2.9$ with $\alpha \geq 10$; for $1 \leq r < 2.9$ with $\alpha > 0$, $\gamma > 0$, and for $r \geq 1.1$ with $(\alpha, \gamma) > 0$.

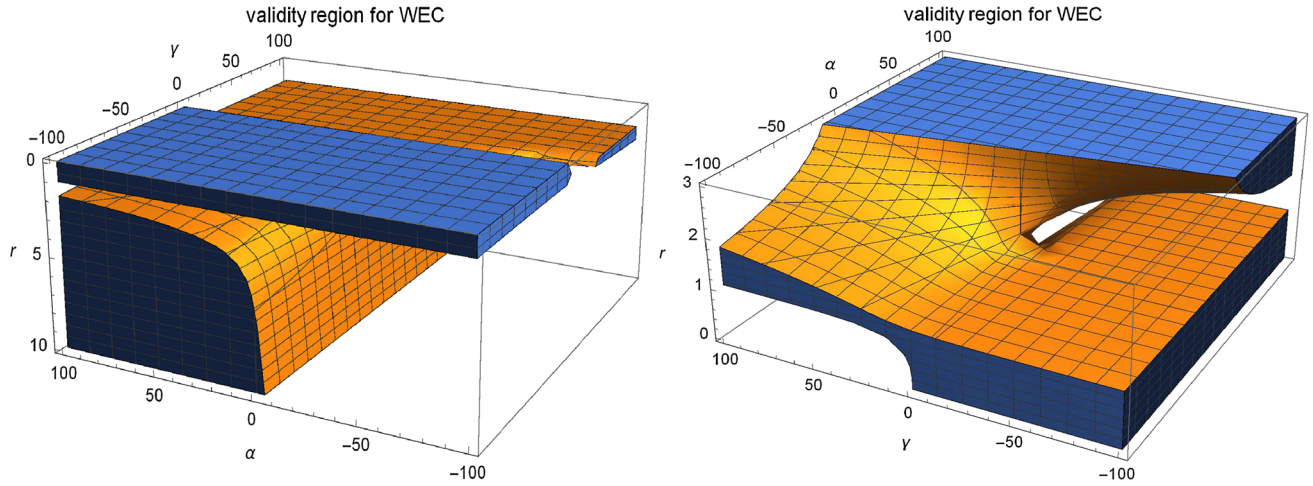

Fig. 1 Validity of WEC for $\lambda = -2$ with $c = 1$ and $m = 1/2$. In the *right plot*, we present the evolution for small r, which is as clear in the *left plot*

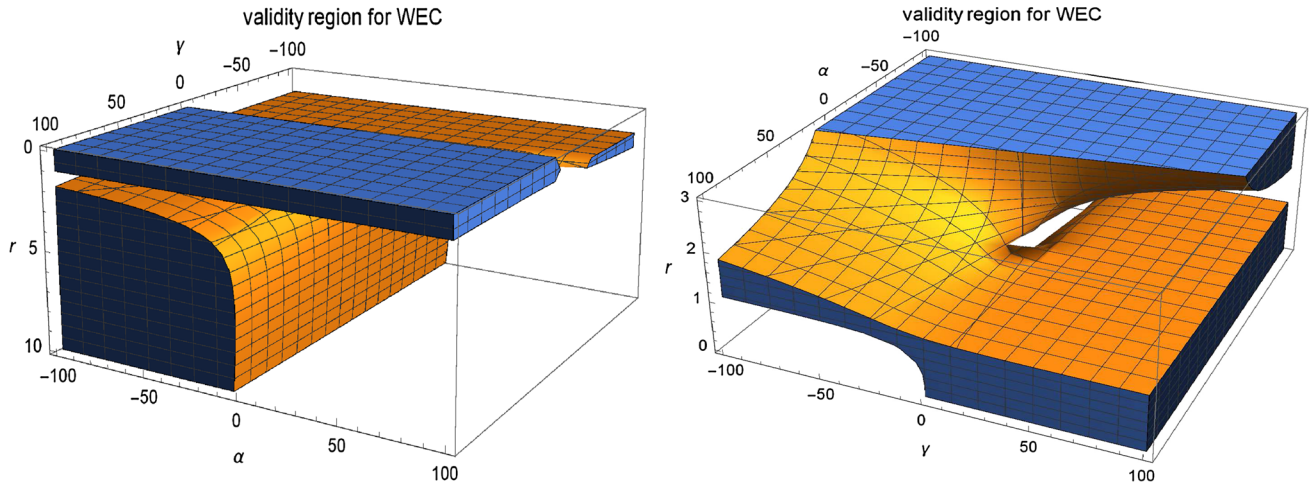

Fig. 2 Validity of WEC for $\lambda = -2$ with $c = 1$ and $m = 1/2$. In the *right plot*, we present the evolution for small r, which is as clear in the *left plot*

In Figs. 3 and 4, we present the evolution of $\rho + p_r > 0$ and $\rho + p_t > 0$ for $\lambda = 2$ and $\lambda = -2$, respectively. We find that there is no region of similarity between $\rho + p_r > 0$ and $\rho + p_t > 0$, though one can find the same validity range for both $\rho > 0$ and $\rho + p_r > 0$. In Fig. 5, we show the plots of the ρ, p_r, and p_t for $c = 1$, $n = 0.5$, $\lambda = 2$, $\alpha = -2$, and $\gamma = -0.1$. It can be seen that both $\rho > 0$ and $p_r > 0$ are satisfied but $p_t > 0$ is violated. Thus, in the anisotropic case, the normal matter threading the wormhole does not satisfy $\rho + p_t > 0$.

- $\beta(r) = r_0^2/r$

For this choice of the shape function, one has to set $m = 1$. The results for this choice are very similar, as the inequalities remain the same, with only a difference with the bounds of the parameters.

- For $\lambda < -1$, WEC is valid if $r \geq 3$ and $\alpha \geq 20$. For small region like $0 < r \leq 1$, we require $\gamma \leq -10$ and for $1 < r < 3$, we require $\alpha > 0$ with $\gamma \geq 10$. $\rho + p_r > 0$ is valid in the following regions:
  $0 < r < 1$ with $\gamma \leq -15$; $r \geq 1.1$ with $\alpha > 0$ and $\gamma > 0$; $r \geq 3$ with $\alpha \geq 15$.
  The validity of $\rho + p_t > 0$ can be met for three cases, i.e.,
  $0 < r < 1$ with $\gamma \geq 15$; $r \geq 1.1$ with $\alpha \leq -5$ and $\gamma < 0$; $r \geq 3$ with $\alpha \leq -15$.
- For $\lambda > -1$, the validity of WEC needs $\alpha \leq -20$ and $r \geq 3$. For a small region like $0 < r < 1$, we require $\gamma \geq 10$ and for $1.1 \leq r < 3$, the validity needs negative

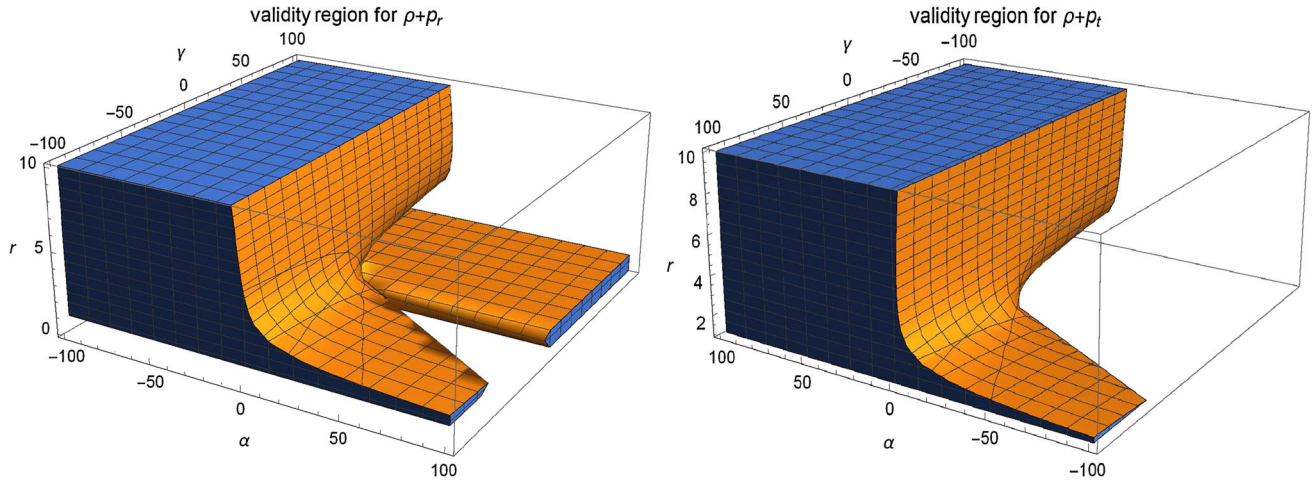

Fig. 3 Validity of $\rho + p_r > 0$ and $\rho + p_t > 0$ for $\lambda = 2$ with $c = 1$ and $m = 1/2$

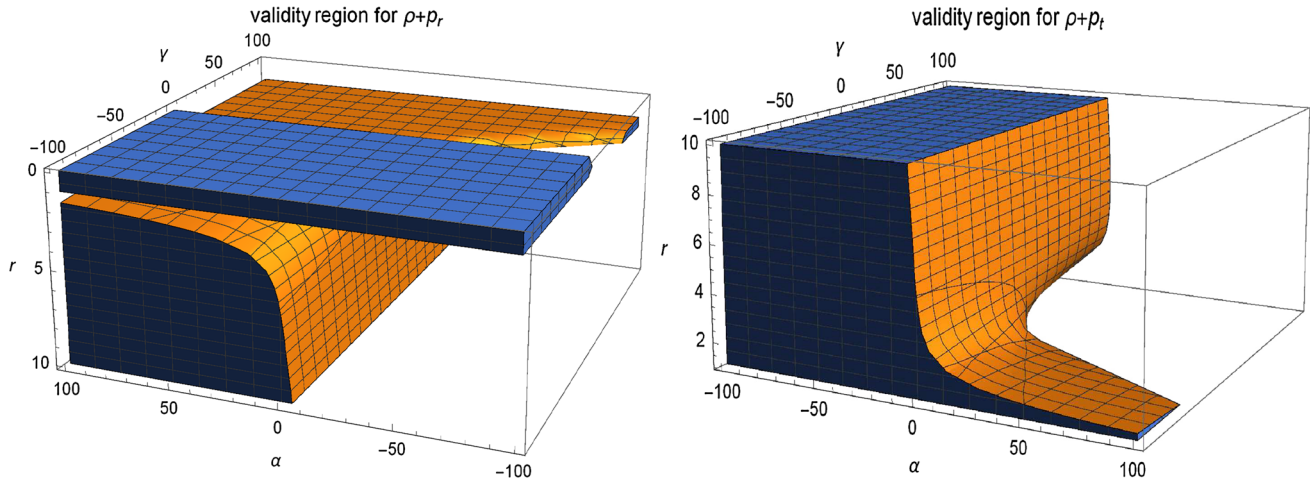

Fig. 4 Validity of $\rho + p_r > 0$ and $\rho + p_t > 0$ for $\lambda = -2$ with $c = 1$ and $m = 1/2$

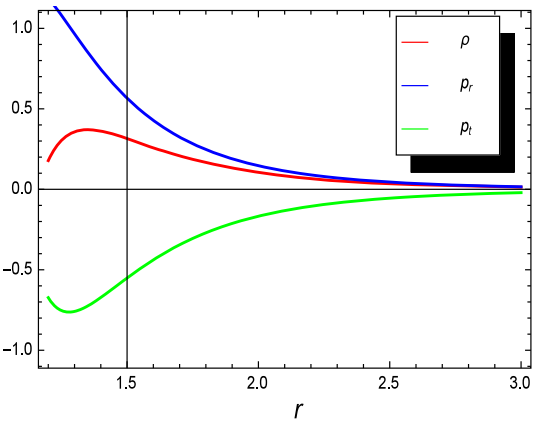

Fig. 5 Evolution of ρ, p_r, and p_t for the anisotropic case with $\lambda = 2$

values of both α and γ, i.e., $\alpha \leq -5$ and $\gamma \leq -20$. NEC with radial pressure can be satisfied for the following ranges depending on the choice of r: if $0 < r < 1$ with $\gamma \geq 15$; if $r \geq 3$, $\alpha \leq -15$; if $1 < r < 3$, $\alpha < -5$, $\gamma < 0$.

In the case of $\rho + p_t > 0$, we can find the validity for the following choices of the parameters: For $0 < r < 1$ with $\gamma \leq -16$; for $r \geq 3$ with $\alpha \geq 10$; for $1 \leq r < 3$ with $\alpha > 0$, $\gamma > 0$.

We would like to mention here that all the choices, like $m = 1, 1/2, -1/2, 1/5$ [47–54], imply the same sort of results as presented in detail for the case of $m = 1/2$. However, the parameter $m = -3$ gives significantly different results.

- $\beta(r) = r_0^2 r^3$

For $m = -3$, we find the shape function of the form $\beta(r) = r_0^2 r^3$, in this case ρ, p_r, and p_t appear to be independent of r. Here, the choice of $\lambda < -1$ results in the following constraints: WEC, $\rho + p_r > 0$ and $\rho + p_t > 0$ are valid only if $\gamma \leq -20$ for all values of α. If one sets $\lambda > -1$ then

the energy conditions are valid only if $\gamma \geq 15$ for all values of α. Hence, for this choice the normal matter threading the wormhole is on cards.

3.2 Equilibrium condition

Now we present some discussion of the equilibrium picture of wormhole solutions. For wormhole solutions, the equilibrium picture can be discussed by taking Tolman–Oppenheimer–Volkov equation given by

$$\frac{\mathrm{d}p_r}{\mathrm{d}r} + \frac{\sigma'}{2}(\rho + p_r) + \frac{2}{r}(p_r - p_t) = 0, \tag{21}$$

which is defined for the metric

$$\mathrm{d}s^2 = e^{\sigma(r)}\mathrm{d}t^2 - e^b\mathrm{d}r^2 - r^2(\mathrm{d}\theta^2 + \sin^2\theta\mathrm{d}\phi^2),$$

where $\sigma(r) = 2a(r)$. This equation describes the equilibrium picture by considering an anisotropic force, arising from anisotropic matter, hydrostatic and gravitational forces that are identified as follows:

$$F_{gf} = -\frac{\sigma'(\sigma + p_r)}{2}, \quad F_{hf} = -\frac{dp_r}{dr}, \quad F_{af} = 2\frac{(p_t - p_r)}{r},$$

and the equilibrium equation takes the form

$$F_{hf} + F_{gf} + F_{af} = 0.$$

In our case, since we have taken $a'(r) = 0$, therefore F_{gf} turns out to be zero and hence the previous equation takes the form

$$F_{hf} + F_{af} = 0.$$

In our case, these forces takes the following form:

$$\begin{aligned} F_{hf} =& \frac{7}{2}r^{-9/2} + \left(\frac{11}{2}\right)\left(\frac{59.5}{3}\right)\alpha r^{-13/2} \\ &- \frac{21}{12}(515.5\gamma)r^{-23/2} + \frac{3}{2}(504\gamma)r^{-10} \\ &- \frac{7}{6}(116.5\alpha)r^{-8}, \end{aligned} \tag{22}$$

$$\begin{aligned} F_{af} =& \frac{2}{r}\left[\frac{681.5\gamma}{6}r^{-21/2} - \frac{4.5}{6}r^{-7/2} - \frac{112\alpha}{6}r^{-11/2}\right. \\ &+ \frac{125\alpha}{6}r^{-7} - \frac{630\gamma}{6}r^{-9} - r^{-7/2} \\ &- \frac{59.5\alpha}{3}r^{-11/2} + \frac{515.5\gamma}{6}r^{-21/2} - \frac{1}{6}r^{-9}(504\gamma \\ &\left. - 116.5\alpha r^2)\right], \end{aligned} \tag{23}$$

where we have used Eqs. (18), (19), and (20) with $m = 1/2$, $n = 3$, $c = 1$, and $\lambda = -2$. For the second case, i.e., $\lambda = 2$, these forces are given by

$$\begin{aligned} F_{hf} =& -\frac{35}{42}r^{-9/2} - \frac{11}{42}(87.5\alpha)r^{-13/2} + \frac{21}{84}(667.5\gamma)r^{-23/2} \\ &- \frac{672}{2}(9\gamma)r^{-10} + \frac{7}{2}(162.5)r^{-8}, \end{aligned} \tag{24}$$

$$\begin{aligned} F_{af} =& \frac{2}{r}\left[-\frac{1}{30}(1327.5\gamma)r^{-21/2} + \frac{7.5}{30}r^{-7/2} + \frac{210\alpha}{30}r^{-11/2}\right. \\ &- \frac{240\alpha}{30}r^{-7} + \frac{1218\gamma}{30}r^{-9} + \frac{5}{21}r^{-7/2} + \frac{87.5\alpha}{21}r^{-11/2} \\ &\left. - \frac{667.5\gamma}{42}r^{-21/2} + \frac{672\gamma}{42}r^{-9} - \frac{162.5\alpha}{42}r^{-7}\right]. \end{aligned} \tag{25}$$

The graphical behavior of these forces is given in Fig. 6. Here we have taken $\alpha = 15$ and $\gamma = 30$ for which the WEC is compatible as discussed previously. The right plot corresponds to the case $\lambda = 2$, while the left plot corresponds to $\lambda = -2$. It can be seen that these forces show similar behaviors but their behaviors are in opposite direction. Therefore, these forces can cancel each other's effect and hence lead to the stability of total configuration. Thus we can conclude that in the case of $f(R, T)$ gravity with anisotropic matter, the wormhole solutions remain stable.

3.3 Isotropic fluid

For this case, we consider $p_r = p_t = p$. Hence, the isotropic condition results in the following equation:

$$\begin{aligned} &\frac{1}{r(1+\lambda)}e^{-b}\left[-12r^3\left(e^b\left(r^2\alpha - 6\gamma\right) - \gamma\right)b'^3 + 120r^4\gamma b'^4\right. \\ &- 12r^2b'^2\left(e^b\left(r^2\alpha - 28\gamma\right) + 36\gamma + 22r^2\gamma b''\right) \\ &+ rb'\left(-e^{2b}r^4 + 28e^br^2\alpha - 12e^{2b}r^2\alpha - 204\gamma + 120e^b\gamma\right. \\ &+ 84e^{2b}\gamma + 4r^2\left(7e^b\left(r^2\alpha - 6\gamma\right) + 18\gamma\right)b'' + 48r^3\gamma b^{(3)}\Big) \\ &+ 2\left(\left(e^b - 1\right)\left(-4e^b\left(7r^2\alpha - 66\gamma\right) - 276\gamma + e^{2b}\left(r^4\right.\right.\right. \\ &\left.\left.\left. - 4r^2\alpha + 12\gamma\right)\right) + 8r^2\left(e^b\left(r^2\alpha - 18\gamma\right) + 18\gamma\right)b'' \\ &\left. + 24r^4\gamma b''^2 - 4r^3\left(e^b\left(r^2\alpha - 6\gamma\right) + 6\gamma\right)b^{(3)}\right)\right] = 0. \end{aligned} \tag{26}$$

Here, one can present the above equation in terms of the shape function $\beta(r)$. It can be seen that Eq. (26) is highly non-linear, which cannot be solved analytically. We use the numerical scheme to solve the above equation and present the results in Figs. 7, 8, and 9. In the left plot of Fig. 7, the evolution of the shape function is shown, which indicates an increasing behavior and the condition $\beta(r) < r$ is obeyed, whereas the right plot represents one of the fundamental wormhole conditions, i.e., the space-time is asymptotically flat, $\beta(r)/r \to 0$ as $r \to \infty$. The throat is located at $r_0 = 0.0932726$ so that

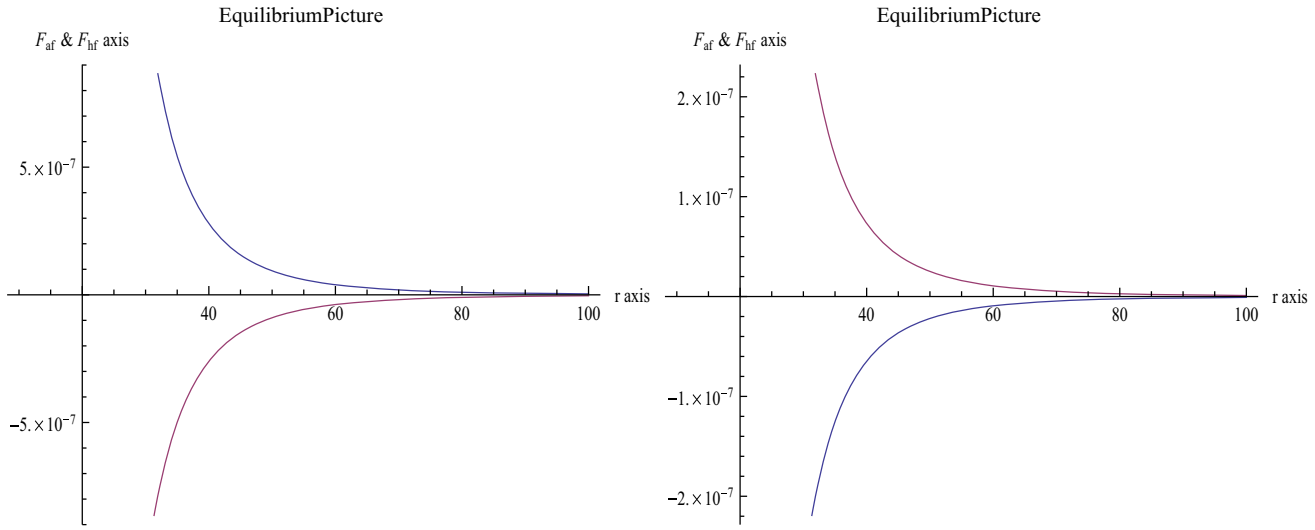

Fig. 6 Evolution of F_{af} and F_{hf} versus r. Herein, we choose $m = 1/2,\ c = 1,\ n = 3,\ \alpha = 15$, and $\gamma = 30$. The *right* and *left plots* correspond to $\lambda = 2$ and $\lambda = -2$, respectively

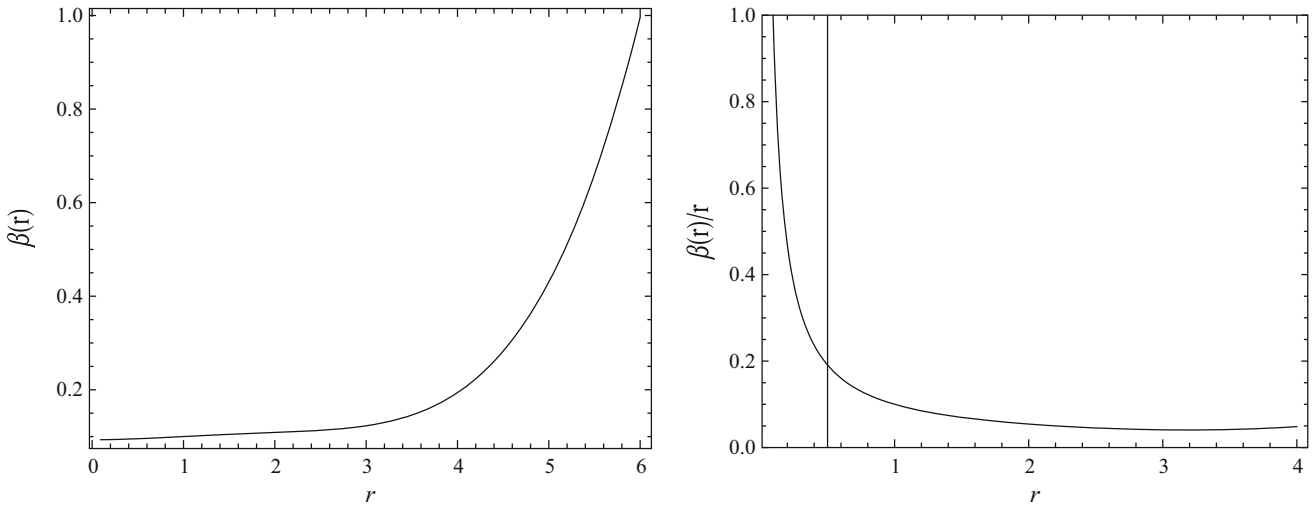

Fig. 7 Evolution of $\beta(r)$ and $\beta(r)/r$ versus r. Herein, for the isotropic case, we set $\lambda = 2, \alpha = 0.6, \gamma = -0.2$

$\beta(r_0) = r_0$. The derivative of the shape function is shown in the right plot of Fig. 8, it can be seen that $\beta'(r_0) = 0.0027559$ so that the condition $\beta'(r_0) < 1$ is satisfied. In the right plot of Fig. 8, we plot the function $\beta(r) - r$, and it is found that $\beta(r) - r < 0$, which validates the condition $1 - \beta(r)/r > 0$. The behavior of WEC and NEC is shown in Fig. 9. It can be seen that $\rho > 0$ throughout the evolution but $\rho + p > 0$ can be met in some particular regions. Thus, a micro wormhole can be formed for this case.

3.4 Specific EoS $p_r = k\rho$

In this case, we apply an EoS involving an energy density and radial pressure, i.e., $p_r = k\rho$. Such an EoS has been applied in $f(R)$ and $f(T)$ gravities [35,47,48] to discuss the wormhole solutions. Using the above defined EoS along with the dynamical equation, we find the following constraint to calculate the shape function:

$$\frac{1}{r(1+\lambda)(1+2\lambda)}e^{-b}\Big[4\gamma(23+62\lambda-k(37+58\lambda)) + e^{3b}(1+k)\Big(r^4(1+2\lambda) - 2r^2(\alpha+3\alpha\lambda)+4(\gamma+4\gamma\lambda)\Big) - 2e^{b}\Big(-30\gamma(-3+5k+8(k-1)\lambda)+r^2 \times\alpha\big(-7-15\lambda+k(5+9\lambda)\big)\Big)$$

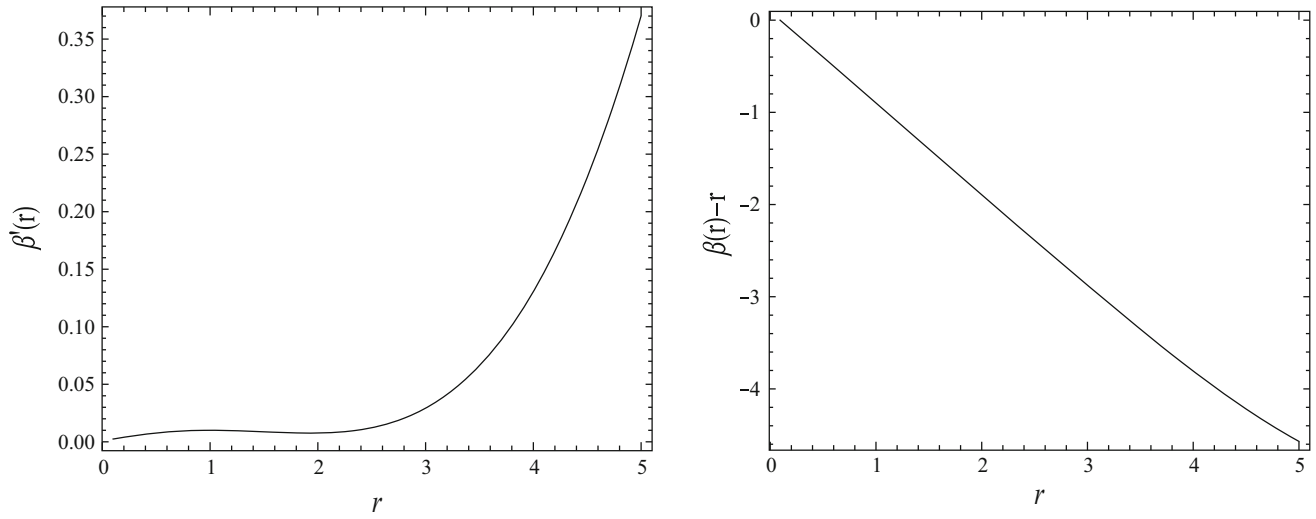

Fig. 8 Evolution of $\beta'(r)$ and $\beta(r) - r$ versus r

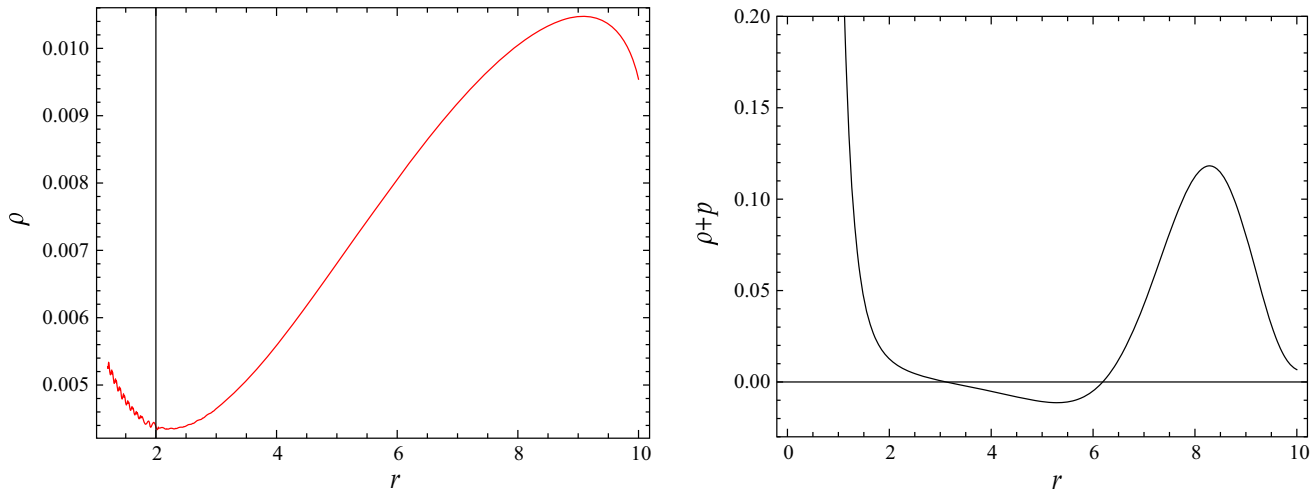

Fig. 9 Evolution of ρ and $\rho + p$ for the isotropic case

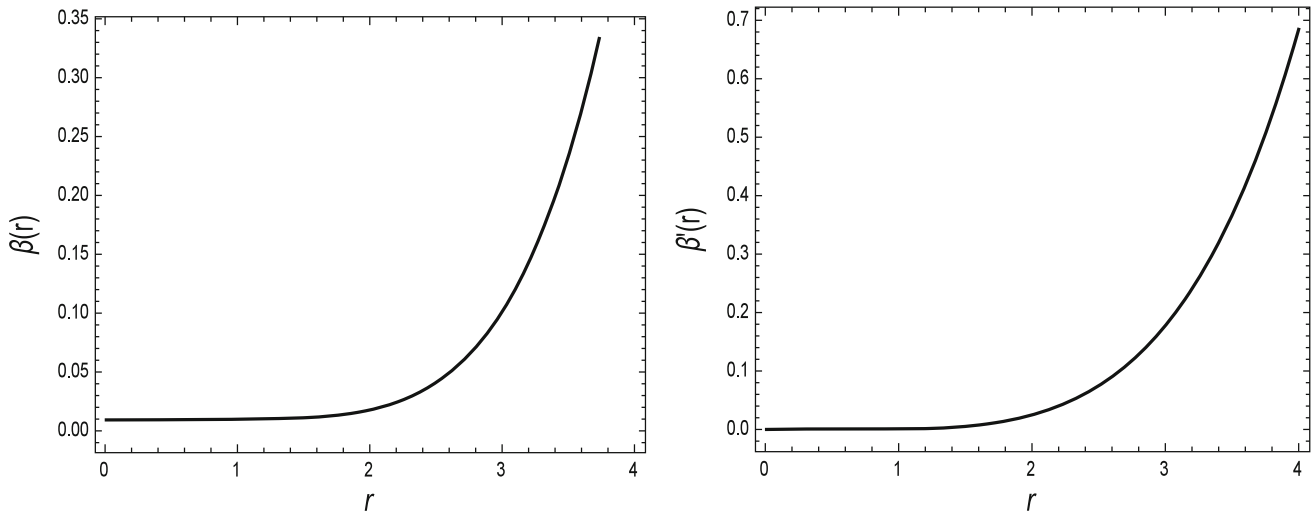

Fig. 10 Evolution of $\beta(r)$ and $\beta'(r)$ versus r. Herein, for the EoS $p_r = k\rho$ we set $\lambda = -2, \alpha = 0.1, \beta = -30, k = 0.001$

$$
\begin{aligned}
&- e^{2b}\Big(- 12r^2\alpha(k-1)(1+2\lambda) + r^4(1+k) \\
&\times (1+2\lambda) + 12\gamma(k(13+22\lambda) - 7 - 18\lambda)\Big) \\
&+ r\Big(r^2\Big(3e^b\big(r^2\alpha - 6\gamma\big)\Big(k(3\lambda+2) - \lambda\Big) \\
&+ 2\gamma\Big(20 + 29\lambda + k\big(32 + 53\lambda\big)\Big)\Big)b'^3 \\
&+ 30r^3\gamma\Big(\lambda - k(2+3\lambda)\Big)b'^4 \\
&+ 6rb'^2\Big(2\gamma(11k - 3 + 14(k-1)\lambda) \\
&- e^b\Big(r^2\alpha(1+k)(1+2\lambda) + 2\gamma(7k - 12 \\
&\times \lambda + 8k\lambda - 3)\Big) + 11r^2\gamma\Big(k(2+3\lambda) - \lambda\Big)b''\Big) \\
&+ b'\Big(12\big(e^b - 1\big)\gamma\Big(8 + k\big(e^b - 1\big)(\lambda - 1) + 13\lambda + 3e^b\lambda\Big) \\
&+ e^b r^2\Big(- 2\alpha\Big(k(4+3\lambda) - 5\lambda\Big) \\
&+ e^b\Big(- 6\alpha(1+k)\lambda + r^2(k + 2k\lambda)\Big)\Big) \\
&+ r^2\Big(- 7e^b\big(r^2\alpha - 6\gamma\big)\Big(k(2+3\lambda) - \lambda\Big) - 6\gamma\big(8 \\
&+ 7\lambda + 9k(2+3\lambda)\big)\Big)b'' + 12r^3\gamma(\lambda - k(2+3\lambda))b^{(3)}\Big) \\
&+ 2r\Big(\Big(6\gamma(4 + 11\lambda - 3k(2+3\lambda)) + e^b \\
&\times \Big(r^2\alpha(4+2k+7\lambda+3k\lambda) + 6\gamma(6k - 4 - 11\lambda + 9k\lambda)\Big)\Big) \\
&\times b'' + 6r^2\gamma\Big(\lambda - k(2+3\lambda)\Big)b''^2 + r\Big(e^b\big(r^2\alpha - 6\gamma\big) \\
&+ 6\gamma\Big)\Big(- \lambda + k(2+3\lambda\Big)b^{(3)}\Big)\Big)\Big] = 0. \qquad (27)
\end{aligned}
$$

Again we transform the above equation in terms of the shape function $\beta(r)$ and employ the numerical approach to show the behavior of flaring out condition and asymptotic flatness. The left plot of Fig. 10 shows $\beta(r)$ as an increasing function of r. In this case, the throat is located at $r = 0.0093117$ with $\beta(r_0) = r_0$ and $\beta'(r_0) < 1$, the behavior of $\beta'(r)$ is shown in the right plot of Fig. 10. Moreover, Fig. 11 shows that our solutions satisfy the flaring out condition, but this solution does not satisfy the asymptotically flat condition, i.e., $\beta(r)/r \to 0$ as $r \to \infty$. The qualitative behavior of ρ and $\rho + p_t$ is shown in Fig. 12. Here, we find that the WEC and NEC are not satisfied, so in this case a realistic wormhole is not possible. Hence, the effective curvature contributions

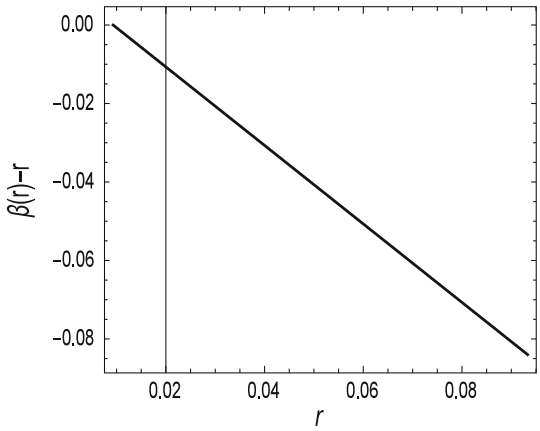

Fig. 11 Evolution of $\beta(r) - r$ for EoS $p_r = k\rho$

in the form of exotic matter help to sustain the wormhole solution.

4 Summary

In GR, wormhole solutions contain a fundamental ingredient, that is, the violation of energy condition in a given space-time. It is taken into consideration that one may impose the principle of a modified Einstein field equation by an effective stress energy-momentum tensor threading the wormholes satisfying the energy conditions and the higher order curvature derivative terms can support the geometries of the non-standard wormholes. In this manuscript, we have investigated whether the ordinary matter can support wormholes in $f(R,T)$ modified gravity. For this purpose, we have examined the behavior of the energy conditions, i.e., WEC and NEC, for three different fluids: barotropic, isotropic, and anisotropic fluids in separate cases.

In the literature, it is pointed out that the theoretical advances in the last decades indicate that pressures within highly compact astrophysical objects are anisotropic, i.e., the radial pressure p_r is not equal to the tangential pressure p_t in such objects. Anisotropic matter is a more general case than the isotropic/barotropic case, so it is interesting to examine the existence of wormholes using such matter contents. In this paper, we examined the existence of wormhole solutions using different matter sources. In the literature, different techniques have been used to discuss wormhole solutions. One technique is to consider the shape function and explore the behavior of the energy conditions and the other technique is to calculate the shape function by taking some assumption for the matter ingredients. In this paper, we are using $f(R,T)$ gravity, which involves coupling of matter and the Ricci scalar; therefore the resulting equations are quite complicated being highly non-linear with six unknowns, namely

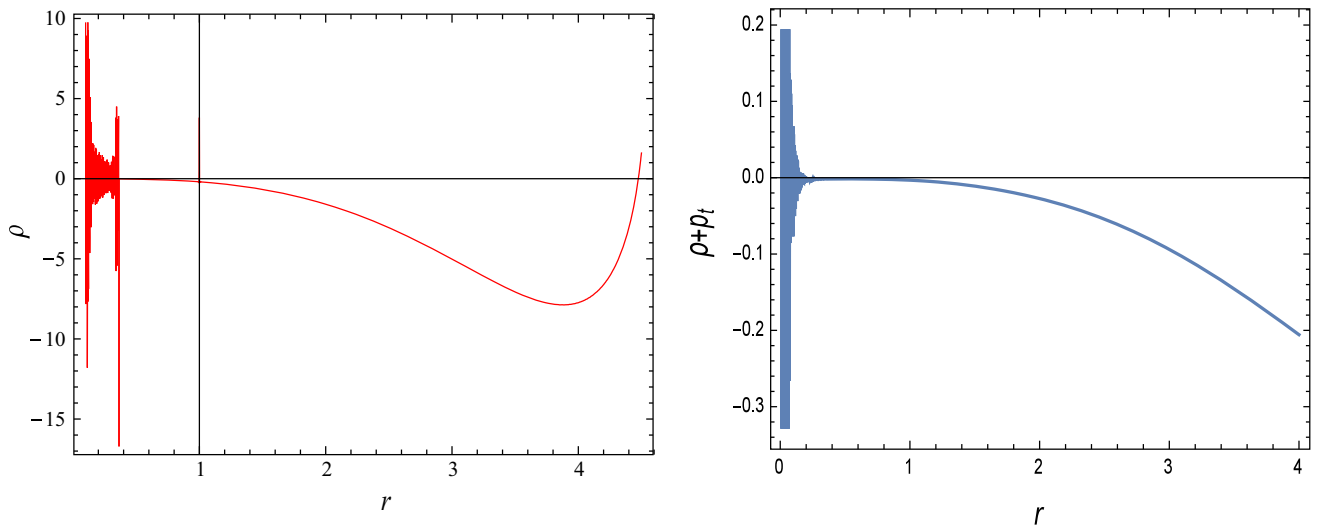

Fig. 12 Evolution of ρ and $\rho + p_t$

ρ, p_t, p_r, b, a, and $f(R)$. Therefore we should make some assumptions.

In the anisotropic case, it is very difficult to explore the form of the shape function from field equations, therefore we explore the behavior of energy condition bounds to check the possible existence of wormholes by assuming a viable form of the shape function. In the other two cases, that is, the barotropic and isotropic matter sources, the equations are less complicated, therefore we have explored the physical behavior of the shape function also. Basically, our purpose is to check whether the coupling of the Ricci scalar with matter field can support the existence of wormhole geometries in such theory. In order to discuss wormhole geometries, we have taken some viable conditions. In all cases, we have assumed a well-defined $f(R)$ model defined as $f(R, T) = f_1(R) + \lambda T$, where $\lambda \in \mathbb{R}$. In the anisotropic case, we have discussed the existence of wormhole solutions by taking a particular choice of the shape function, whereas for the other two cases we have solved the field equation numerically to investigate the behavior of the shape function. In the case of an anisotropic fluid, the behaviors of the energy constraints have been discussed for two cases of the coupling parameter: $\lambda > 0$ and $\lambda < -1$. For $\lambda < -1$, it is observed that the WEC is valid for positive values of α, while the small validity regions can be found when $\alpha < 0$. For $\lambda < -1$, it is observed that the validity regions for WEC can be increased by taking large values of α. For $\lambda > 0$, the validity of WEC requires a negative range of α, whereas small validity regions can be found for $\alpha > 0$.

First, in our result, wormhole solutions exist but these are not realistic or physically reasonable as one cannot find the similarity regions for the compatibility of the energy bounds, although it is a mathematically well-defined problem. Our results are consistent with the work already available in the literature [55,56]. Our results are also similar to that obtained in simple $f(R)$ gravity [35] (that is, the case $\lambda = 0$). It is interesting to mention here that in these studies, both energy bounds, i.e., WEC and DEC, are violated in the anisotropic and isotropic cases; only in the barotropic case there are some regions where these conditions are compatible, while in our case, only the DEC energy bound is violated for the anisotropic case. In other cases, these conditions remain compatible for some specific ranges of parameters. This difference of result may have arisen due to the presence of a curvature–matter coupling term.

In the literature, the existence of wormhole solutions in curvature–matter coupled gravity has been discussed by Bertolami and Ferreira [57] and Garcia and Lobo [58]. In both these studies, one has presented a very restricted analysis in this sense that the authors have used linear functions as $f(R)$ model, and also very specific ranges of free parameters have been discussed. They showed that the wormhole solutions obtained are well behaved, satisfying DEC when λ is positive and increasing. It is interesting to mention here that our results are more comprehensive than these previous works, as we have explored the behavior of the functions involved and the existence of a wormhole by taking all possible ranges of the involved parameters (specifically λ can take any value). Furthermore, we have used the Starobinsky model that represents R^n extension ($n \geq 3$) instead of linear functions. Garcia and Lobo [59] also discussed the wormhole existence in curvature–matter coupling gravity by taking a linear $f(R)$ model with positive increasing ansatz for density, which is not a physically reasonable choice for the density on cosmological grounds (as it should be a decreasing function).

We have also investigated the equilibrium picture of the wormhole solutions found with anisotropic matter in this theory of gravity. It is seen that the wormhole solutions are sta-

ble as the equilibrium condition involving hydrostatic and anisotropic forces is satisfied. In the case of barotropic and isotropic fluids, we have explored the dynamics of the shape function by solving equations numerically. From the graphical illustrations of the shape function, it is seen that in the isotropic case, all the necessary conditions like asymptotically flatness and the flaring out constraint are satisfied, which indicates that the obtained micro wormhole is realistic and viable. In the case of a barotropic fluid, the asymptotic flatness condition is incompatible; therefore, a realistic wormhole solution does not exist. It is interesting to find wormhole solutions without exotic matter by considering some other different $f(R, T)$ models in this theory of gravity.

Funded by SCOAP[3].

References

1. S. Perlmutter et al., Astrophys. J. **483**, 565 (1997)
2. S. Perlmutter et al., Nature **391**, 51 (1998)
3. S. Perlmutter et al., Astrophys. J. **517**, 565 (1999)
4. S. Nojiri, S.D. Odintsov, Phys. Rep. **505**, 59 (2011)
5. A.A. Starobinsky, Phys. Lett. B **91**, 99 (1980)
6. R. Ferraro, F. Fiorini, Phys. Rev. D **75**, 084031 (2007)
7. M. Zubair, Int. J. Modern. Phys. D **25**, 1650057 (2016)
8. S. Carroll et al., Phys. Rev. D **71**, 063513 (2005)
9. G. Cognola, Phys. Rev. D **73**, 084007 (2006)
10. A.G. Agnese, M. La Camera, Phys. Rev. D **51**, 2011 (1995)
11. G. Kofinas, N.E. Saridakis, Phys. Rev. D **90**, 084044 (2014)
12. T. Harko et al., Phys. Rev. D **84**, 024020 (2011)
13. M.J.S. Houndjo et al., Int. J. Mod. Phys. D **21**, 1250003 (2012)
14. M.J.S. Houndjo et al., Int. J. Mod. Phys. **2**, 1250024 (2012)
15. M. Sharif, M. Zubair, JCAP **03**, 028 (2012)
16. C.P. Singh, V. Singh, Gen. Relat. Gravit. **46**, 1696 (2014)
17. Mubasher et al., Eur. Phys. J. C **72**, 1999 (2012)
18. M. Sharif, M. Zubair, J. Phys. Soc. Jpn. **82**, 064001 (2013)
19. H. Shabani, M. Farhoudi, Phys. Rev. D **88**, 044048 (2013)
20. H. Shabani, M. Farhoudi, ibid. Phys. Rev. D **90**, 044031 (2014)
21. A.F. Santos, Mod. Phys. Lett. A **28**, 1350141 (2013)
22. M. Sharif, M. Zubair, Gen. Relat. Gravit. **46**, 1723 (2014)
23. M. Zubair, I. Noureen, Eur. Phys. J. C **75**, 265 (2015)
24. I. Noureen, M. Zubair, Eur. Phys. J. C **75**, 62 (2015)
25. I. Noureen, M. Zubair, A.A. Bhatti, G. Abbas, Eur. Phys. J. C **75**, 323 (2015)
26. Alvarenga et al., Phys. Rev. D **87**, 103526 (2013)
27. Baffou et al., Astrophys. Space Sci. **356**, 173 (2015)
28. M.F. Shamir, Eur. Phys. J. C **75**, 354 (2015)
29. P.H.R.S. Moraes, Eur. Phys. J. C **75**, 168 (2015)
30. M. Zubair et al., Astrophys. Space Sci. **361**, 8 (2016)
31. M. Zubair, M. Syed, Ali Hassan. Astrophys. Space Sci. **361**, 149 (2016)
32. H. Shahbani, arXiv:1604.04616v1
33. A. Einstein, N. Rosen, Phys. Rev. **48**, 73 (1935)
34. F.S.N. Lobo, M.A. Oliveira, Phys. Rev. D **80**, 104012 (2009)
35. M. Sharif, Z. Zahra, Astrophys. Space Sci. **348**, 275 (2013)
36. M.S. Morris, K.S. Thorne, Am. J. Phys. **56**, 395 (1988)
37. M.S. Morris, K.S. Throne, U. Yurtseve, Phys. Rev. Lett. **61**, 1446 (1988)
38. T. Azizi, Int. J. Theor. Phys. **52**, 3486 (2013)
39. L.D., Landau, E.M. Lifshitz, *The Classical Theory of Fields* (Butterworth-Heinemann, 2002)
40. Alvarenga et al., J. Mod. Phys. **4**, 130 (2013)
41. M. Sharif, M. Zubair, J. Phys. Soc. Jpn. **82**, 014002 (2013)
42. M. Ozkan, Y. Pang, Class. Quantum Grav. **31**, 205004 (2014)
43. U.D. Goswami, K. Deka, Int. J. Mod. Phys. D **22**, 1350083 (2013)
44. A.A. Starobinsky, JETP Lett. **86**, 157 (2007)
45. A.V. Frolov, Phys. Rev. Lett. **101**, 061103 (2008)
46. W. Hu, I. Sawicki, Phys. Rev. D **76**, 064004 (2007)
47. M. Jamil, D. Momeni, R. Myrzakulov, Eur. Phys. J. C **73**, 2267 (2013)
48. C.G. Boehmer, T. Harko, F.S.N. Lobo, Phys. Rev. D **85**, 044033 (2012)
49. P. Pavlovic, M. Sossich, Eur. Phys. J. C **75**, 117 (2015)
50. J.B. Dent, S. Dutta, E.N. Saridakis, J. Cosmol. Astropart. Phys. **009**, 1101 (2011)
51. T.P. Sotiriou, B. Li, J.D. Barrow, Phys. Rev. D **83**, 104030 (2011)
52. B. Li, T.P. Sotiriou, J.D. Barrow, Phys. Rev. D **83**, 104017 (2011)
53. Y. Zhang, H. Li, Y. Gong, Z.H. Zhu, J. Cosmol. Astropart. Phys. **015**, 1107 (2011)
54. S. Bhattacharya, S. Chakraborty, arXiv:1506.03968v2
55. M.R. Mehdizadeh, M.K. Zangeneh, F.S.N. Lobo, Phys. Rev. D **91**, 084004 (2015)
56. M. Jamil, D. Momeni, R. Myrzakulov, Eur. Phys. J. C **73**, 2267 (2013)
57. O. Bertolami, R.Z. Ferreira, Phys. Rev. D **85**, 104050 (2012)
58. N.M. Garcia, F.S.N. Lobo, Phys. Rev. D **82**, 104018 (2010)
59. N.M. Garcia, F.S.N. Lobo, Class. Quantum Grav. **28**, 085018 (2011)